HAL
archives-ouvertes.fr

Dispersion mechanisms of carbon black in an elastomer matrix

Véronique Collin, Edith Peuvrel-Disdier

▶ **To cite this version:**

Véronique Collin, Edith Peuvrel-Disdier. Dispersion mechanisms of carbon black in an elastomer matrix. Elastomery, 2005, 9 (No Special), pp.Pages 9-15. <hal-00663087>

HAL Id: hal-00663087

https://hal-mines-paristech.archives-ouvertes.fr/hal-00663087

Submitted on 26 Jan 2012

HAL is a multi-disciplinary open access archive for the deposit and dissemination of scientific research documents, whether they are published or not. The documents may come from teaching and research institutions in France or abroad, or from public or private research centers.

L'archive ouverte pluridisciplinaire **HAL**, est destinée au dépôt et à la diffusion de documents scientifiques de niveau recherche, publiés ou non, émanant des établissements d'enseignement et de recherche français ou étrangers, des laboratoires publics ou privés.

Dispersion mechanisms of carbon black in an elastomer matrix

Véronique Collin and Edith Peuvrel-Disdier *
Ecole des Mines de Paris
Centre de Mise en Forme des Matériaux, UMR CNRS / Ecole des Mines de Paris N° 7635
BP207, 06904 Sophia-Antipolis, France
* Author to whom correspondence should be adressed: edith.disdier@ensmp.fr

Introduction

The mixing of carbon black or silica pellets and a matrix implies distinct phases e.g., (i) incorporation, (ii) distribution and (iii) dispersion [Nak81]. To disperse implies to reduce the pellet size (around the millimeter) down to the aggregate size (a few tens of nanometers). This size is necessary to ensure the reinforcement of the matrix (see for example [Ham00]). Dispersion and distribution processes will define the dispersion state of the carbon black in the final product and thus its end-use properties. A prediction of the mixing process (after the incorporation step) including a local evolution of the size distribution of the carbon black pellets implies an exact modeling of the flow and temperature fields in the mixer and a good knowledge of the laws governing the dispersion mechanisms. Although the mixing of filler particles and a matrix is a common operation, the mechanisms responsible for the size reduction of the filler are not fully understood. One way to improve this knowledge would be to be able to observe inside the mixer what happens, which is not possible. Rheo-optical techniques recently appeared as a relevant tool to investigate in-situ dispersion but in a simpler flow (shear). However most studies concerned the dispersion of fillers in low viscosity matrices [RFM90-91, YMF97-98, SN01, PMF03].

The objective of the present work was to identify, understand and model the flow-induced dispersion mechanisms of carbon black in an uncured elastomer. This was achieved by using a transparent counter-rotating shear cell which enables to perform in-situ optical observations of the dispersion mechanisms under shear. The work presented in this paper reports on the two main mechanisms of dispersion which are erosion and rupture.

Experimental part

Counter-rotating shear cell

To observe the dispersion of carbon black pellets while the suspending matrix is submitted to shear, a specially designed transparent counter-rotating shear cell was developed and used in this study. This apparatus consists of two glass plates rotating in opposite directions. The principle of the counter-rotating geometry is represented in Figure 1.b. Each plate is driven by an independent motor. The advantage of this geometry is that the relative velocities of the two plates can be adjusted so that the velocity of a given particle can be set to zero in the reference framework of the laboratory. This allows to observe the behaviour of a particle suspended in a matrix under shear either for a certain period of time at a given shear rate or while increasing the shear rate.

Figure 1

This device is equipped with powerful motors in order to be able to shear high viscosity fluids like elastomers.

A heating system permits to control the temperature up to 180°C. It consists of a metallic heating plate (see Figure 2) against which the lower plate stands and an upper oven equipped with resistances. The heating of the sample is performed by conduction through the direct contact between the lower plate and the heating plate. The upper oven heats the shear cell by radiation. Its aim is to keep a constant temperature of the air around the sample in order to avoid temperature gradients. The upper part of the oven is constituted by two separate parts. This allows to mount the upper oven when the sample is introduced between the two glass plates.

Figure 2

Observations during shear are performed via an optical microscope. They are recorded by a CCD camera and a video recorder. During a dispersion experiment, any change in the carbon black pellet size during shear is quantified using an image analysis system (Visilog 5.3 software).

Experimental conditions for dispersion experiments

Samples consist of sandwiches of two thin films of elastomer with a few pellets randomly placed in between (see Figure 3). Thin films of elastomers are prepared by compression-molding. After insertion of the sample between the two glass plates, the gap is adjusted in order to observe the wetting of the filler by the matrix to ensure a good macroscopic contact between the pellet and the matrix. Care was taken not to apply any additional external pressure. For this reason, after setting the gap, the sample was left at rest for 45 minutes in order to ensure a good temperature control and more specifically a good relaxation of the elastomer before the application of a shear flow. Experiments were conducted at 140°C.

Figure 3

The gap dimension relatively to the pellet dimension was chosen in order that the pellet was only subjected to the applied macroscopic shear stress (shear rate multiplied by the corresponding viscosity of the matrix) and not to any additional stresses due to the vicinity of the shear cell walls [MBB05]. We determined in another study using a 3D finite element modeling of the flow cell that the particle diameter relatively to the gap of the shear cell should not exceed a 0.4 factor in order to avoid any stress contribution due to the vicinity of the wall. This condition was satisfied.

Materials

The dispersion mechanisms of a N234 carbon black (from Cabot) were investigated. This carbon black is typically used in the tire industry. Carbon black pellets were not submitted to any particular thermal treatment before their use.

Dispersion was studied in a styrene-butadiene rubber (SBR 25E from Michelin).

The rheological characteristics of the elastomer was measured by oscillatory experiments using a RMS800 Rheometrics rheometer (25 mm diameter). Measurements were performed in the linear regime. The complex viscosity (η^*) is plotted versus frequency on Figure 4. Rheological data are shown at 140°C, temperature at which rheo-optical experiments were performed.

Figure 4

Since the infiltration of a fluid inside a pellet does affect the dispersion mechanism [YMF98], the infiltration property of the elastomer matrix was estimated using silica (Z1115MP from Rhodia) instead of carbon black pellets. Elastomers although very viscous do infiltrate into porous filler particles [ACR04]. Infiltration kinetics can be measured in silica pellets using an optical microscope since as soon as the matrix penetrates into the porous silica, the impregnated part becomes transparent. The non-wetted part appears opaque because of the strong light scattering due to the air contained in the pores. Infiltration kinetics were measured in the counter-rotating device in the absence of shear (measurements performed at rest). The principle of these measurements is described in details in Astruc et al. [ACR04]. Such measurements show that SBR is characterised by a very slow infiltration process and no infiltration is assumed to take place in the carbon black pellet within the time considered in dispersion experiments.

Background

Motion of a particle suspended in a Newtonian fluid under shear

The motion of an axisymmetric particle, suspended in a Newtonian matrix under simple shear flow, consists of a spin around its axis of symmetry and the precession of this axis around the vorticity axis of the undisturbed flow [Jef22]. The macroscopic applied shear rate ($\dot{\gamma}$) can be directly related to the period of the precession rotation (T) by Jeffery:

$$\dot{\gamma} = \frac{2\pi}{T}\left(r_p + r_p^{-1}\right) \qquad (1)$$

with r_p the particle aspect ratio.

The flow field induces tensile stresses on the particle, which are maximal at 45° and at 225° in Newtonian fluids [Bre64]. The hydrodynamic stress acting on the pellet was calculated by Bagster and Tomi [BT74] for an isolated, impermeable and uniform sphere in a simple shear flow field. All fragments within the pellet experience a maximum hydrodynamic force at 45° during the sphere rotation, given by:

$$F_H = \frac{5}{2}\pi R^2 \eta \dot{\gamma} \sin^2 \psi_0 \qquad (2)$$

where R is the sphere radius, η is the fluid viscosity, $\dot{\gamma}$ is the shear rate and ψ_0 is the angle which describes the size of the fragment on which the force is applied relatively to the total sphere.

Rupture

Rupture is characterised by the sudden fracture of the pellet into a few pieces. It occurs when the hydrodynamic force F_H exceeds the cohesive force F_{COH} between the fragment and the remainder of the pellet [BC58, MKe62]. For this reason, the prediction of the breakage condition implies the balance of these two components, the hydrodynamic stress acting on the pellet and the cohesive strength.

Two different models were used to describe the cohesion of the pellet which give rise to different rupture mechanisms. The first model of planar fracture assumes that the rupture occurs along some planar surface which divides the pellet into two spherical caps. In this case, the hydrodynamic stress is equal to:

$$\sigma_H = \frac{5}{2}\eta\dot{\gamma} \qquad (3)$$

Rumpf [Rum62] proposed that the cohesive stress for an homogeneous pellet is a function of the mean interparticle force H between particles constituting the pellet and the size d of these particles:

$$\sigma_{COH} \propto H/d^2 \qquad (4)$$

Rupture should happen as soon as:

$$\eta\dot{\gamma} \geq \text{const}\,\frac{H}{d^2} \qquad (5)$$

This model predicts that critical conditions for rupture should be independent of the pellet size:

$$\tau_C^{\text{Rupture}} = \text{const.} \qquad (6)$$

The second model of irregular fracture [HFM92] considers an heterogeneous structure of the pellet and that the force bonding the fragment to the parent pellet depends on the number of bonds N_b. Thus, the cohesive resisting force is given by:

$$F_{Coh} = H\,N_b \qquad (7)$$

Bohin *et al.* [BMF96] suggested that the number of bonds scales with the size of the potential fragment:

$$N_b \propto R^m \text{ with } m \in [0,2] \qquad (8)$$

m=0 corresponds to the case of high porosity pellets where a potential fragment should be connected to the parent pellet by a relatively small number of connecting bonds, whereas m=2 corresponds to dense pellets where the number of connecting bonds should scale with the surface area. Thus in high porosity pellets, rupture should occur whenever:

$$\eta\dot{\gamma} \geq \text{const.}/R^2 \qquad (9)$$

Whereas for dense pellets, the condition should be:

$$\eta\dot{\gamma} \geq \text{const.} \qquad (10)$$

In this irregular fracture model, the dependence or not of the critical conditions for rupture on the pellet size should be a function of the pellet density.

Kendall [Ken88] proposed that the rupture propagates along internal defects. In this case the cohesion strength is related to the defect size.

The effect of the pellet size on the critical shear stress for rupture was addressed by Horwatt et al. [HFM92] who numerically generated different types of structures and examined the two types of fractures. The relationship between the cluster size and the critical stress for rupture depends on the structural organisation.

No systematic experimental determination of this criterion was reported in the literature.

Erosion models

Erosion is a progressive mechanism where small fragments are continuously detached from the periphery of the parent pellet by the flow of the matrix around the pellet. This mechanism was first identified by Shiga and Furuta [SF85]. There exists a few models to predict the erosion process of a pellet, models which were validated by experimental measurements. Most experiments concern artificially built pellets of silica or carbon black suspended in a low viscosity Newtonian matrix. The different laws are recalled below:

Kao and Mason [KM75] proposed for cohesionless pellets that the number of spherical particles removed from the periphery of the pellet is proportional to the macroscopic shear stress $\eta_0\dot{\gamma}$ applied to the matrix at a given point on the surface of the matrix. This model predicts a linear dependence of the eroded volume with strain:

$$R_0^3 - R_t^3 = c_1\,\dot{\gamma}\,t \qquad (11)$$

where R_0 is the initial pellet radius, R_t is the pellet radius at time t, c_1 is a constant which includes the viscosity parameter η_0 and $\dot{\gamma}$ is the shear rate. Seyvet *et al.* [SN01] confirmed the validity of this law for cohesive carbon black pellets in a Newtonian fluid.

Powell and Mason [PM82] presented a second erosion model by adding that the rate of fragment detachment is proportional to the surface area of the pellet. This gives a linear variation of the eroded thickness with strain:

$$R_0 - R_t = c_2\ b\ \dot{\gamma}\ t \qquad (12)$$

where c_2 is a constant which includes the viscosity parameter and b the size of the detached fragments.

Later, Rwei *et al.* [RMF91] studied the erosion of artificially compacted cohesive carbon black or silica pellets. Their description of the process is based on Powell and Mason's model and assumes that the size of the eroded fragments is proportional to the size of the parent pellet (hypothesis based on their experimental observations). A logarithm law was proposed:

$$\ln(R_t/R_0) = -c_3\ \dot{\gamma}\ t \qquad (13)$$

where c_3 is a constant which includes the viscosity parameter. For short dispersion times, a linear variation of the relative eroded thickness versus the quantity of strain units is obtained:

$$\frac{R_0 - R_t}{R_0} = c_4\ \dot{\gamma}\ t \qquad (14)$$

The constant c_4 was found to be shear stress dependent but independent of the initial pellet size.

Bohin *et al.* [BMF96] and recently Scurati *et al.* [SFM02] postulated that the rate of erosion should be proportional to the excess of hydrodynamic force acting on a fragment relative to its cohesive strength. Their model predicts a faster erosion for larger pellets and for higher shear stresses.

In these different models, key parameters for erosion appear to be the initial cluster size, the size of the detached fragment, time or strain, shear rate and/or shear stress. The fact that the matrix may infiltrate the porous substrate is not included in these models although it is a key parameter (modification of cohesion and effect on dispersion mechanisms). In the case of Newtonian matrices, it was shown that the ratio of the thickness of the infiltrated layer relatively to the depth at which the shear is transmitted determines the erosion mechanism and in particular erosion kinetics [YMF97-98]. For large infiltration depths, erosion is slow, whereas for small infiltration depths, erosion is fast and proceeds through the detachment of fragments corresponding to the infiltration depth.

Results [Col04, CPD05]

Identification of dispersion mechanisms

Various mechanisms of dispersion were identified in the SBR matrix. Examples of mechanisms observed in the case of the N234 carbon black are shown in Figure 5.

Figure 5

The two main mechanisms of dispersion which are erosion and rupture were observed in the case of isolated carbon black pellets in the SBR matrix. Debonding (characterised by the sudden detachment of the matrix from the pellet) was also observed in this matrix. Debonding can be at the origin of the pellet rupture [Ast01] as observed for the N234 carbon black. In the case of more concentrated systems, the collision between pellets is also at the origin of dispersion (see Figure 6).

Figure 6

Quantification of the rupture mechanism

The condition for rupture was determined by increasing gradually the shear rate until the rupture mechanism is observed. The shear rate at which the rupture is observed is referred as the critical shear rate for rupture ($\dot{\gamma}_C^R$). The critical shear stress for rupture corresponds to the shear rate multiplied by the viscosity at that shear rate ($\tau_C^{Rupture} = \eta\left(\dot{\gamma}_C^R\right)\ \dot{\gamma}_C^R$). Pellets with as possible spherical shapes were selected. The criterion was determined for different sizes of pellets. The critical shear stress for rupture was found to be inversely proportional to the pellet size (see Figure 7):

$$\tau_C^{rupture} \propto {}^{1}\!/_{R_0} \qquad (15)$$

The meaning of this critical shear stress for rupture is that:

If $\tau < \tau_C^{Rupture}\left(R_0\right)$ ➠ the pellet of radius R is not fractured.

If $\tau > \tau_C^{Rupture}\left(R_0\right)$ ➠ the pellet (size R) is ruptured by the action of the shear stress.

The fact that the critical shear stress for rupture is not constant is in contradiction with some theoretical models [HFM92].

Figure 7

Quantification of the erosion process

Erosion kinetics were measured by following the gradual reduction of the cluster size as a function of time or strain. The total time for erosion does depend on the pellet

size. The erosion of a larger pellet is longer. The use of the model proposed by Kao and Mason [KM75] allows to gather all erosion kinetics measured for different initial pellet sizes on a single curve (Figure 8). The model predicts that, whatever the initial pellet size, the eroded volume per strain unit ($\gamma = \dot{\gamma}\, t$) is constant:

$$R_0^3 - R(t)^3 = k\,\dot{\gamma}\,t \quad \text{with} \quad k \neq f(R_0) \qquad (16)$$

Figure 8

One important parameter during mixing is the applied shear stress. The effect of this parameter was investigated by measuring erosion kinetics at different shear rates (see Figure 9). It was found that the erosion rate does depend on the applied shear stress. A higher shear stress results in a faster erosion. The dependence of the erosion rate with the shear stress is given by the following relationship:

$$k = \alpha\left(\tau - \tau_C^{Erosion}\right) \qquad (17)$$

with α characterizing the erosion efficiency and $\tau_C^{Erosion}$ the critical shear stress for erosion.

Figure 9

The integration of this dependence into the erosion law does enable to describe the erosion process as a single law taking into account the effect of the initial pellet size and the applied shear stress with two erosion parameters characteristic of the filler/matrix system (α and $\tau_C^{Erosion}$) :

$$R_0^3 - R(t)^3 = \alpha\left(\tau - \tau_C^E\right)\dot{\gamma}\,t \qquad (18)$$

Conclusion

For the first time, rupture and erosion mechanisms of isolated carbon black pellets were quantified in an elastomeric matrix under shear conditions.

A criterion for rupture and an erosion law were determined:

- Rupture was shown to be characterised by a critical shear stress which depends on the pellet size.

- Erosion was found to proceed via the detachment of a constant eroded volume per strain unit whatever the initial size is. The eroded volume does depend on the applied shear stress.

This set of criterion and law describes the dispersion of a carbon black pellet in an elastomeric matrix due to the hydrodynamic stress subjected to the pellet. This provides a set of pertinent and workable equations to predict the pellet size evolution of a single pellet under shear conditions. This set of criterion and law for dispersion was used to define a model for dispersion to be incorporated in a complete modelling of mixing in a batch mixer [ALA05, AAL05].

References

[ACR04] Astruc, M., Collin, V., Rusch, S., Navard, P., Peuvrel-Disdier, E., J. Appl. Polym. Sci. 91, 2004, 3292

[AAL05] Alsteens, B., Avalosse, T., Legat, V., Elastomery, 2005, in this volume

[ALA05] Alsteens, B., Legat, V., Avalosse, T., Elastomery, 2005, in this volume

[Ast01] Astruc, M., Etude rhéo-optique des mécanismes de dispersion de mélanges sous cisaillement simple: 1. Mélanges concentrés de polymères immiscibles, 2. Mélanges polymères-charges poreuses, Thèse de Doctorat, Ecole des Mines de Paris, Sophia Antipolis, France, 2001

[BC58] Bolen, W. R., Colwell, R. E., Intensive mixing, SPE Journal, August, 1958, 24

[BMF96] Bohin, F., Manas-Zloczower, I., Feke, D. L., Chem. Eng. Sci., 51(23), 1996, 5193

[Bre64] Brenner, H., Chem. Eng. Sci., 19, 1964, 631

[BT74] Bagster, D. F., Tomi, D., Chem. Eng. Sci., 29, 1974, 1773

[Col04] Collin V., Etude rhéo-optique des mécanismes de dispersion du noir de carbone dans des élastomères, Thèse de Doctorat, Ecole des Mines de Paris, Sophia Antipolis, France, 2004.

[CPD05] Collin, V., Peuvrel-Disdier, E., In-situ study of dispersion mechanisms of carbon black in an elastomer under shear, submitted to J. Applied Polym Sci.

[Ham00] Hamed, G.R., Rubber Chemical and Technology 73(3), 2000, 524

[HFM92] Horwatt, S. W., Feke, D. L., Manas-Zloczower, I., Powder Technol., 72(1), 1992, 113

[Jef22] Jeffery, G.B., Proc. Roy. Soc. London, A 102, 1922, 161

[Ken88] Kendall, K., Powder Metallurgy, 31(1), 1988, 28

[KM75] Kao, S. V., Mason, S. G., Nature, 253, 1975, 619-621

[MBB05] Ménard, P., Bikard, J., Budtova T., Peuvrel-Disdier E., 3D numerical simulation of the behaviour of spherical particles suspended in a newtonian fluid submitted to a simple shear, in preparation.

[MKe62] Mc Kelvey, J. M., Polymer Processing, John Wiley & Son, Inc, NY, 1962
[Nak81] Nakajima, N., Rubber Chemistry Technology 54, 1981, 266
[PM82] Powell, R. L., Mason, S. G., AIChe Journal, 28(2), 1982, 286
[PMF03] Pomchaitaward, C., Manas-Zloczower, I., Feke, D. L., Chem. Eng. Sci., 58, 2003, 1859
[RFM90] Rwei, S. P., Feke, D. L., Manas-Zloczower, I., Polym. Eng. Sci. 30, 1990, 701
[RFM91] Rwei, S. P., Feke, D. L., Manas-Zloczower, I., Polym. Eng. Sci. 31, 1991, 558
[Rum62] Rumpf, H., Agglomeration, W. A. Knepper ed., New York, 1962
[SF85] Shiga, S. and Furuta M., Rubber Chemistry and Technology 85, 1985, 1
[SFM02] Scurati, A., Feke, D.L., Manas-Zloczower, I., Model and analysis of kinetics erosion in simple shear flows, Rubber Division Meeting, Savannah, Georgia, april 28th –may 1st , (2002)
[SN01] Seyvet, O., Navard, P., J. Applied Polym. Sci., 80, 2001, 1627
[YMF97] Yamada, H., Manas-Zloczower, I. and Feke, D. L., Powder Technol., 92, 1997, 163
[YMF98] Yamada, H., Manas-Zloczower, I. and Feke, D. L., Rubber Chem. Technol., 71, 1998, 3

Acknowledgements

This work is part of a project supported by the European Community in the framework of the "Competitive and Sustainable Growth" program. The authors wish to thank all the partners including ThyssenKrupp Elastomertechnik, Michelin, Snecma Propulsion Solide, Optigrade-TechPro, Polyflow, Cesame (U.C. Louvain) and T.U. Lodz for their collaboration in this project.

Captions for the figures:

Figure 1: Principle of the counter-rotating geometry

(a.) Relatively to a classical rotating shear cell

(b.) In the counter-rotating geometry, the particle velocity can be fixed to zero relatively to the laboratory framework while the matrix is subjected to shear. In an usual rotating shear cell, the particle is moving.

Figure 2: Counter-rotating device

(a.) Schematic representation of the global apparatus

(b.) View of the device

Figure 3: Sample preparation

Figure 4: Rheological characteristics (η^*) of SBR at 140°C

Figure 5: Dispersion mechanisms of carbon black N234 in SBR under shear

Figure 6: Example of dispersion induced by the collision of two carbon black pellets

Figure 7: Critical shear stress for rupture versus the inverse of the pellet radius. System N234 in SBR at 140°C

Figure 8: Erosion kinetics plotted as the eroded volume versus strain for different initial pellet sizes

Figure 9: Effect of the applied shear rate on erosion kinetics. System N234 in SBR at 140°C.

a.

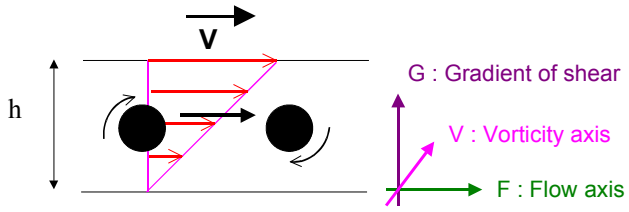
V
h
G : Gradient of shear
V : Vorticity axis
F : Flow axis

b.

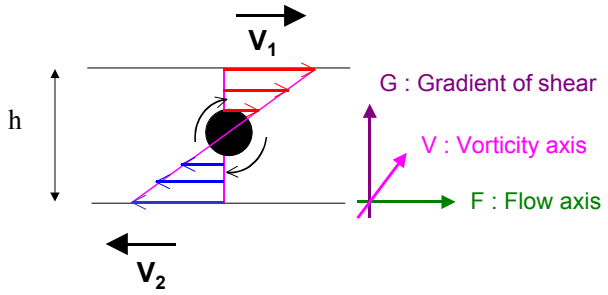
V1
h
G : Gradient of shear
V : Vorticity axis
F : Flow axis
V2

Figure 1

a.

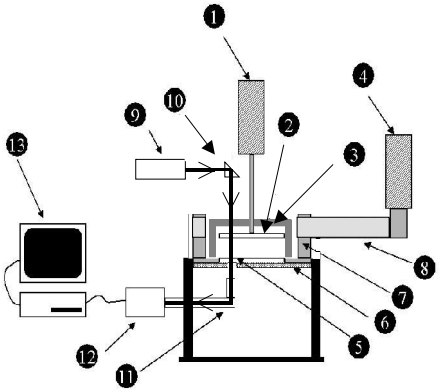

1 : upper motor
2 : upper plate
3 : upper oven (in two parts)
4 : lower motor
5 : lower plate
6 : lower oven
7 : moving support of the lower plate
8 : driving belt
9 : lighting system
10 : prism
11 : microscope
12 : camera
13: monitor and video recorder

b.

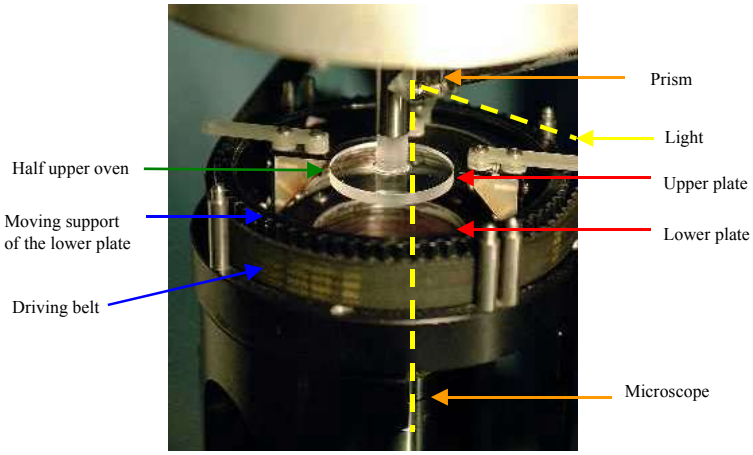

Figure 2

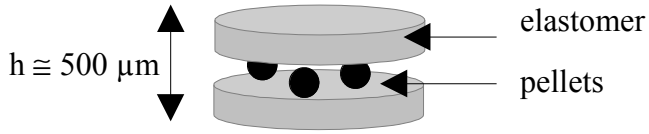

Figure 3

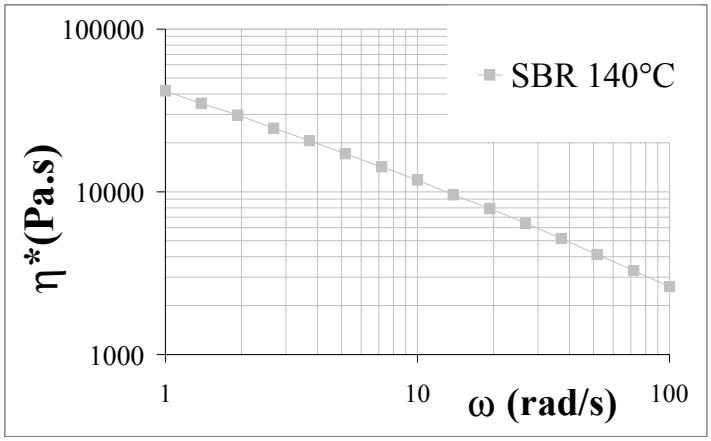

Figure 4

Three different mechanisms were identified in **SBR**:		
Rupture	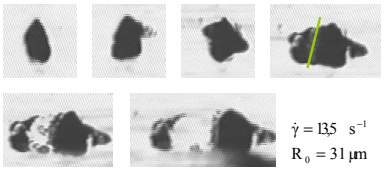	Rupture is an abrupt process characterised by the break-up of the pellet into two or a few large pieces. It happens suddenly when a critical shear rate is attained.
Erosion	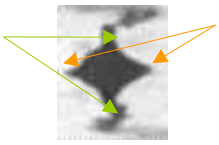	Erosion, which is a more gradual process, is characterised by the detachment of small fragments from the outer surface of the cluster.
Debonding	(1) 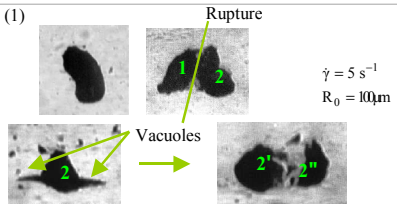 (2) 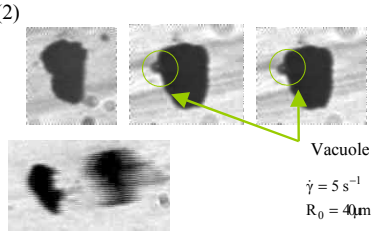	We also identified the mechanism of debonding characterised by the sudden detachment of the matrix from the filler. It can happen after a rupture (1) or spontaneously (2) at higher shear rates. Debonding for the carbon black N234 always induces the rupture of the cluster.

Figure 5

Collision	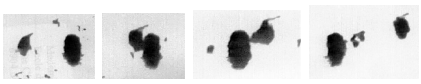	After collision, a fragment is detached from the parent cluster.

Figure 6

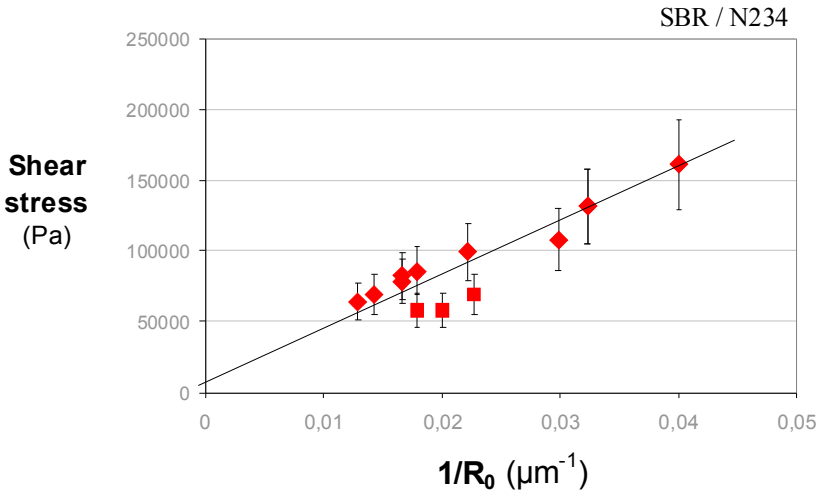
SBR / N234
Shear stress (Pa)
250000
200000
150000
100000
50000
0
0
0,01
0,02
0,03
0,04
0,05
1/R0 (µm-1)

Figure 7

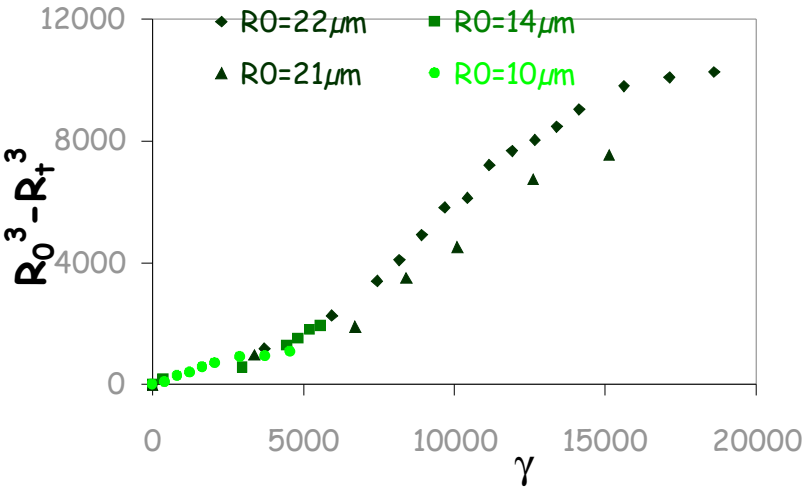
12000
8000
4000
0
0
5000
10000
15000
20000
γ
$R_0^3 - R_t^3$
R0=22μm
R0=14μm
R0=21μm
R0=10μm

Figure 8

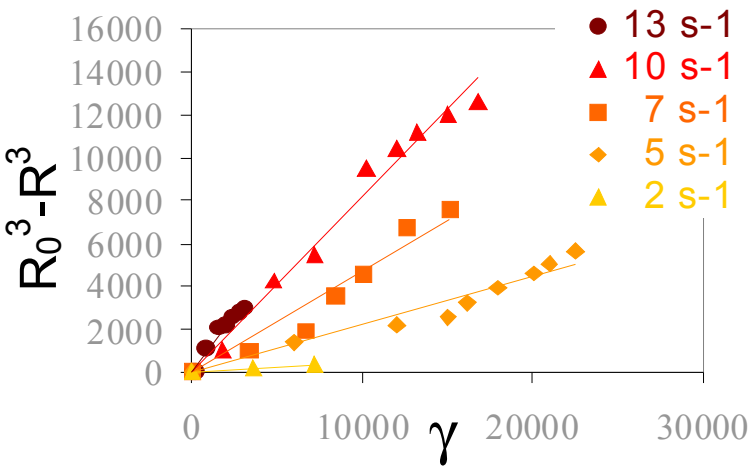
16000
14000
12000
10000
8000
6000
4000
2000
0
$R_0^3-R^3$
0
10000
γ
20000
30000
13 s-1
10 s-1
7 s-1
5 s-1
2 s-1

Figure 9